Contents lists available at ScienceDirect

Plant Physiology and Biochemistry

journal homepage: www.elsevier.com

Short communication

Ancient signal for nitrogen status sensing in the green lineage: Functional evidence of CDPK repertoire in *Ostreococcus tauri*

Gonzalo Caló, Dana Scheidegger, Giselle M.A. Martínez-Noël, Graciela L. Salerno*

Instituto de Investigaciones en Biodiversidad y Biotecnología (INBIOTEC-CONICET) and Centro de Investigaciones Biológicas, FIBA, 7600 Mar Del Plata, Argentina

ARTICLE INFO

Article history:
Received 16 February 2017
Received in revised form 7 July 2017
Accepted 7 July 2017
Available online xxx

Keywords:
Calcium signalling
CDPK
Ostreococcus tauri
Prasinophytes
Nitrogen starvation

ABSTRACT

Calcium-dependent protein kinases (CDPKs) regulate plant development and many stress signalling pathways through the complex cytosolic [Ca^{2+}] signalling. The genome of *Ostreococcus tauri* (*Ot*), a model prasinophyte organism that is on the base of the green lineage, harbours three sequences homologous to those encoding plant CDPKs with the three characteristic conserved domains (protein kinase, autoregulatory/autoinhibitory, and regulatory domain). Phylogenetic and structural analyses revealed that putative *Ot*CDPK proteins are closely related to CDPKs from other Chlorophytes. We functionally characterised the first marine picophytoeukaryote *CDPK* gene (*OtCDPK*1) and showed that the expression of the three *OtCDPK* genes is up-regulated by nitrogen depletion. We conclude that CDPK signalling pathway might have originated early in the green lineage and may play a key role in prasinophytes by sensing macronutrient changes in the marine environment.

1. Introduction

Calcium ion (Ca^{2+}) is a ubiquitous and conserved second messenger in all eukaryotes. Specific Ca^{2+} signatures are decoded by several sensor proteins that trigger changes in metabolism by modulating gene expression. Among these sensors, Ca^{2+}-dependent protein kinases (CDPKs) are confined to extant members of plants (Viridiplantae) and to a few apicomplexans (supergroup SAR) (Billker et al., 2009). Plant CDPKs participate in the response to many abiotic and biotic stresses (Wan et al., 2007; Tsai et al., 2007; Hu et al., 2016; Zeng et al., 2017), and in metabolic and physiological processes, such as starch accumulation, root development, abscisic acid response, stomata closure, pollen tube growth, and seed development (Frattini et al., 1999; Kumar et al., 2004). Comprehensive phylogenetic and evolutionary analyses have concluded that CDPKs might have predated the first land plants and that the Chlorophya-Streptophyta split played a key role in the evolution of CDPKs (Hamel et al., 2014; Delaux et al., 2015).

CDPKs are normally called sensor/responder proteins because they harbour both sensing function through Ca^{2+}-binding and protein kinase activity as responder within a single gene product (Sanders et al., 2002). Typical CDPKs have four characteristic domains: the highly variable N-terminal region, the Ser/Thr kinase catalytic domain, the autoregulatory/autoinhibitory portion (a pseudosubstrate sequence), and the calmodulin-like region (regulatory domains that contain EF-hands for binding calcium ions) (Harmon et al., 2000). CDPKs are activated by binding to calcium *via* the calmodulin-like domain leading to a conformational change in the autoinhibitory domain, which results in the exposure of the active site (Harper et al., 1991; Harmon et al., 2000). The N-terminal extension is a variable region, associated to protein localization and *in vivo* phosphorylation (Schulz et al., 2013). This domain may contain myristoylation and palmotylation sites that are implicated in CDPK-membrane associations (Cheng et al., 2002; Simeunovic et al., 2016).

In unicellular green algae, CDPK protein purification, activity determination, and/or protein detection have been reported in chlorophytes belonging to the classes Chlorophyceae (*Dunaliella tertiolecta*, *D. salina* and *Chlamydomonas moewusii*) (Guo and Roux, 1990; Yuasa and Muto, 1992; Yuasa et al., 1995; Siderius et al., 1997) and Ulvophyceae (*Ventricaria ventricosa*) (Sugiyama et al., 2000), and in the streptophyte *Closterium ehrenbergii*, belonging to the class Conjugatophyceae (Yuasa and Hashimoto, 2006). The first algal CDPK encoding sequence was reported for *D. tertiolecta* (Pinontoan et al., 2000). Recent studies in *Chlamydomonas reinhardtii* showed that CDPK3 isoform plays a role in flagellar biogenesis (Liang and Pan, 2013), and CDPK1 and CDPK3 are transcriptionally regulated in response to nutrient starvation (Motiwalla et al., 2014). However, there is no comprehensive characterisation of the CDPK family from unicellular algae of the genera *Micromonas, Bathycoccus* and *Ostreococcus*, placed in Mamiellophyceae (prasinophyte clade II), the largest clade of prasinophytes (Leliaert et al., 2012). This group diverged earlier in the green lineage and is composed by unicellular picoeukaryotes

* Corresponding author. Instituto de Investigaciones en Biodiversidad y Biotecnología (INBIOTEC-CONICET) and Centro de Investigaciones Biológicas, FIBA, Vieytes 3103, 7600 Mar Del Plata, Argentina.
Email address: gsalerno@fiba.org.ar (G.L. Salerno)

http://dx.doi.org/10.1016/j.plaphy.2017.07.009
0981-9428/

that play a major role in biogeochemical cycling in the oceans, especially in oligotrophic areas (Li, 1994). *Ostreococcus tauri* is the smallest known free-living eukaryote with a single mitochondrion and chloroplast, and a compact nuclear genome (Derelle et al., 2006).

In the present study, we compared CDPKs from *O. tauri* (*Ot*CDPKs) with known CDPKs from plants and other green algae, and functionally characterised the highest transcribed isoform. We also present evidence that the expression of the three members of the *OtCDPK* family is up-regulated by nitrogen deficiency, suggesting that they may be involved in the low-nitrogen stress response, and supporting the ancient origin of the CDPK signal transduction pathway.

2. Materials and methods

2.1. Biological material and culture conditions

Ostreococcus tauri OTTH0595 (RCC745) was purchased from the Roscoff Culture Collection (RCC). Cells were grown in K medium (Keller et al., 1987) supplemented with f/2 vitamin solution in the presence of penicillin 25 μg mL^{-1}, neomycin 20 μg mL^{-1} and kanamycin 25 μg mL^{-1}, at 20 ± 1 °C and under 60 μE illumination with a 12 h/12 h photoperiod (light/dark). For nitrogen-deficient experiments, cells were cultured in K medium lacking $NaNO_3$ and NH_4Cl, which were replaced by equal quantities of NaCl.

Escherichia coli DH5α and BL21(λDE3):pLysS (Novagen) strains were grown in Luria Bertani medium supplemented with 50 μg.mL^{-1}carbenicillin (Martínez-Noël et al., 2007).

2.2. RNA isolation and quantitative reverse transcription

O. tauri cells harvested at exponential phase were sonicated at 40 W in an ice bath (10 cycles of 10 s, followed by a 10 s pause each) (Sonics Vibra Cell, Sonics and Materials Inc.). Total RNA was isolated using the RNeasy plant mini kit (Qiagen). A post-extraction DNase digest was performed at 37 °C for 1 h using DNase Turbo (Ambion, Life Technologies).

Quantitative reverse transcription PCR (qRT-PCR) was performed in a two-step assay. In the first step, single-stranded cDNA was made from treated total RNA (3 μg) and MMLV (Moloney murine leukemia virus) reverse transcriptase (Promega) and random hexamers (Promega). To enable experimentation on *OtCDPK*s differential expression (second step), qPCR primers for the three genes and two commonly used endogenous control genes (*OtGAPDH* and *Ot18S-rDNA*, GenBank accession numbers CAL52398 and Y15814, respectively) were designed (Supplemental Table 1). qPCR assays were performed using a Step One real time PCR system (Applied Biosystems) in a Micro Amp Fast Optical 48-well reaction plate (0.1 mL), with 15 μL reaction volume containing 1× Power Sybr Green PCR Master Mix (Thermo Fisher), 0.2 μM of each primer and 1.5 μL of cDNA. Cycling parameters were: one cycle of 95 °C for 10 min, 40 cycles of 95 °C for 15 s followed by 40 cycles of 54 °C for 1 min. Real-time data were collected during the annealing/extension step. Each primer set was tested for amplification specificity by analysing the melting-curve with the following conditions: 95 °C for 15 s, 60 °C for 1 min and 95 °C for 15 s. Secondary PCR products and primer dimers were not detected in the melting-curve profile. The linear range for each primer set was calculated using serially diluted (1–1:100) cDNA for each one. The relative standard curve method between the experimental conditions was assessed using qPCR. *OtGAPDH* and *Ot18S rDNA* expression were used as internal controls for standardizing experimental data from *OtCDPK* genes. The expression of *OtNAR2* (accession number XM_003081480, coding for a nitrate high-affinity transporter accessory protein) was used as positive control in the nitrogen depletion experiment.

2.3. Cloning and expression of OtCDPK1 coding sequence

The *OtCDPK1* full-length coding sequence (1458 bp) (accession number XP_003078254) was PCR-amplified using specific primers (Supplemental Table 1), cloned into a pGEM®-T Easy vector (Promega), ascertained by sequencing, and finally sub-cloned between the *Bgl*II/*Hind*III sites of the expression vector pRSET-A (Invitrogen). The construct was transferred to *E. coli* BL21(λDE3):pLysS cells (Novagen) and the expression of the recombinant protein was induced with 0.5 mM isopropyl ß-D-thiogalactoside. After 16-h induction at 18 °C, cells were harvested and homogenised. The fusion protein (His_6:*Ot*CDPK1) was partially purified by Co^{2+}-affinity chromatography (TALON® resin, Clontech), dialyzed, and concentrated for further characterisation (Martínez-Noël et al., 2007). Proteins from the cell-free *E. coli* extracts and partially purified His_6:*Ot*CDPK1 were quantified according to Bradford (1976). Immunoanalysis was carried out by using recombinant potato CDPK antibodies (Chico et al., 2002), which were a kind gift from R. Ulloa (INGEBI-CONICET, Argentina) after polypeptide separation by sodium dodecyl sulfate polyacrylamide gel electrophoresis (SDS-PAGE), transfer to a membrane, and visualization with luminol (Biolumina Pb-L).

2.4. CDPK activity assay

CDPK activity was assayed according to Chico et al. (2002) in a 60-μL reaction mixture containing 20 mM Tris–HCl (pH 7.5), 10 mM $MgCl_2$, 10 mM β-mercaptoethanol, 50 μM [γ-^{32}P]-ATP (specific activity 122 Bq-$pmol^{-1}$, New England Nuclear), and 25 μM Syntide-2 (Sigma-Aldrich) with the addition of 1 mM EGTA or 100 μM $CaCl_2$. After incubation at 30 °C for 10 min, a 40-μL aliquot was placed on P81 paper. The reaction was stopped with 75 mM phosphoric acid and radioactivity was determined in a scintillation counter.

2.5. Sequence and phylogenetic analysis

BLASTp searches in the *O. tauri* OTH95 genome (http://www.jgi.doe.gov) were performed using *Triticum aestivum* CDPK (*Ta*CDPK1, accession Q6KCK6) as query. Multiple protein sequence alignments were conducted using ClustalW from the MEGA5 software (Tamura et al., 2011) and consensus sequence logos were made using the WebLogo 3 server (Crooks et al., 2004). Domain organization was studied using ScanProsite database (de Castro et al., 2006).

Subcellular localization signals were predicted using BaCelLo (www.biocomp.unibo.it/bacello) (Pierleoni et al., 2006), Mitoprot-II (www.ihg.gsf.de/ihg/mitoprot), (Claros and Vincens, 1996), ChloroP (www.cbs.dtu.dk/services/ChloroP) (Emanuelsson et al., 1999), Protein Prowler 1.2 (http://bioinf.scmb.uq.edu.au:8080/pprowler_webapp_1-2) (Bodén and Hawkins, 2005; Hawkins and Bodén, 2006), TargetP1.1 (http://www.cbs.dtu.dk/services/TargetP/) (Emanuelsson et al., 2007), and WoLF PSORT (https://wolfpsort.hgc.jp/) (Horton et al., 2007).

Phylogenetic analysis was carried out with Neighbour-Joining approach using MEGA5 software (Tamura et al., 2011), using 1000 replicates in a non-parametric bootstrapping to assess tree branching support. The myristoylation and palmitoylation sites were predicted by Myristoylator (Bologna et al., 2004) and CSS-Palm 2.0 (Ren et al., 2008).

3. Results and discussion

3.1. Identification of CDPK encoding genes in the O. tauri genome

Previous work reported diverse numbers of putative CDPK sequences (0, 15, 2 and 3) in the *O. tauri* genome (Ye et al., 2009; Wang et al., 2010; Hindle et al., 2014; Hamel et al., 2014). We retrieved only three sequences homologous to *CDPK* genes (Ot03g03440, Ot09g03470 and Ot15g01210 locus) located in chromosomes 3, 9 and 15, respectively, with one intron each in the N-terminal region (Fig. 1), whose deduced amino-acid sequences (*Ot*CDPK1, *Ot*CDPK2 and *Ot*CDPK3) had the typical CDPK structure containing an N-terminal highly variable region, a protein kinase domain (PKD), an autoinhibitory region, and a calmodulin-like domain with four EF-hands (Supplemental Fig. 1). BALSTp searches using wheat *Ta*CDPK1 as query also retrieved three additional sequences that lack the typical CDPK structure (Supplemental Fig. 2). Regarding *Ot*CDPK2, our analysis differs from that reported by Hamel et al. (2014) who predicted only three EF-hand motifs.

Subcellular localization signals on the primary amino-acid sequence of *Ot*CDPKs were investigated using computational methods. The tools used predicted that *Ot*CDPK1 is likely to be a cytosolic protein; while, *Ot*CDPK2 and *Ot*CDPK3 may be targeted to mitochondria (Supplemental Table 2). In addition to the N-myristoylation site in *Ot*CDPK2 sequence reported by Hamel et al. (2014), we found a putative S-palmitoylation site in *Ot*CDPK1. In plants, these posttranslational modifications have diverse biological functions in signalling, associated with proteins targeted to membrane locations. *N*-myristoylation promotes protein-membrane and protein–protein interaction and *N*-palmitoylation can stabilize the interaction between protein and membrane (Martín and Busconi, 2001). Palmitoylation and myristoylation seems to be correlated, being the myristoylation event necessary to allow palmitoylation (Martín and Busconi, 2001; Mohanta et al., 2017). Thus, it is more likely that *Ot*CDPK2 and not *Ot*CDPK3 may be a membrane-associated protein. Subcellular distribution enables CDPKs to sense the local Ca^{2+} concentration and to interact with their targets (Simeunovic et al., 2016).

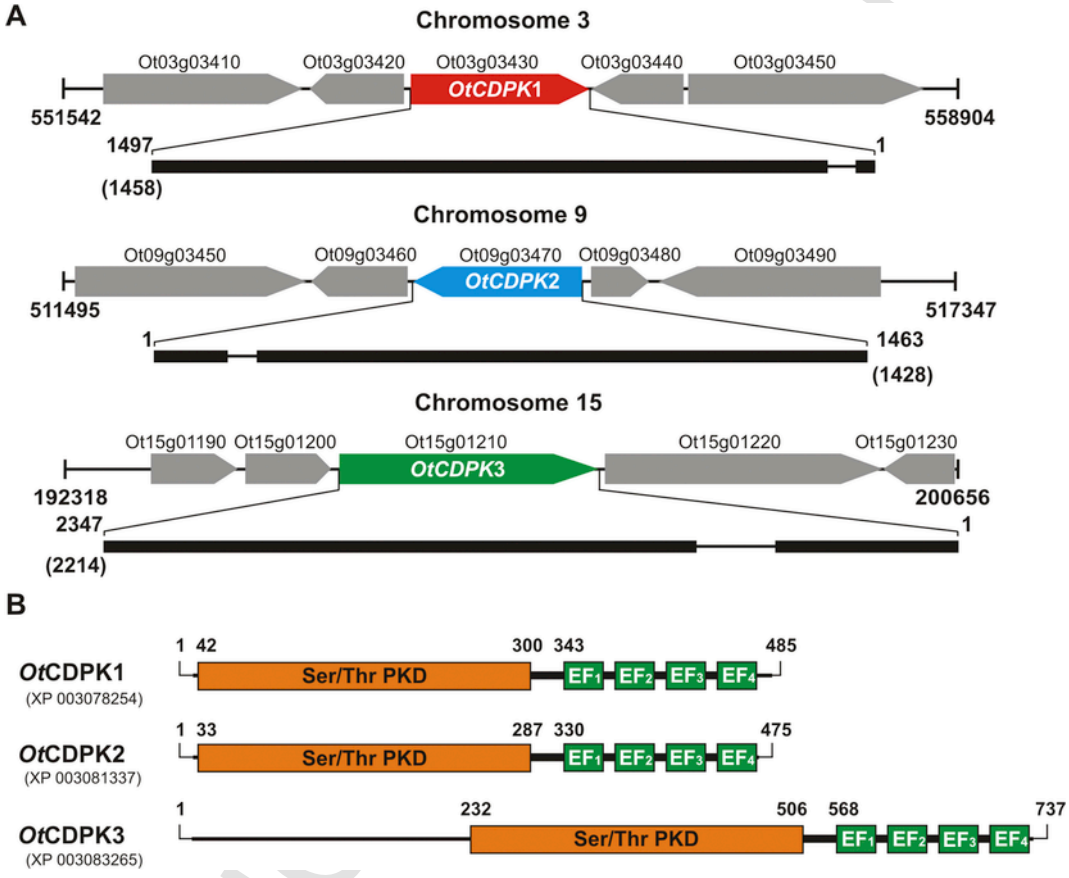

Fig. 1. CDPK family in *Ostreococcus tauri* OTTH0595 genome. BLASTp searches in the *O. tauri* genome (http://genome.jgi.doe.gov/) were carried out using *Triticum aestivum TaCDPK1* (Q6KCK6) full-length sequence as query. **A)** Genomic region vicinity and gene structure of the three putative *OtCDPK*s. Ot03g03430, Ot09g03470, and Ot15g01210 correspond to the open reading frames named *OtCDPK1*, *OtCDPK*2, and *OtCDPK*3, respectively. Adjacent sequences are annotated as: Ot03g03410, DNA-binding protein jumonji/RBP2/SMCY that contains JmjC domain; Ot03g03420, hypothetical protein; Ot03g03440, FKBP-type peptidyl-prolyl cis-trans isomerase; Ot03g03450, MLH_TETTH Micronuclear linker histone polyprotein; Ot09g03450, meltrins, fertilins and related Zn-dependent metalloproteinases of the ADAMs family; Ot09g03460, MGC53924 protein, O-methyltransferase, family 3; Ot09g03480, hypothetical protein; Ot09g03490, splicing coactivator SRm160/300, subunit SRm160 (contains PWI domain); Ot15g01190, 60s ribosomal protein L15/L27; Ot15g01200, hypothetical protein; Ot15g01220, cytoplasmic exosomal RNA helicase SKI2, DEAD-box superfamily; Ot15g01230, oxygen-evolving complex-related. Fine black lines and black bars represent introns and exons, respectively. **B)** Structure of the three putative *Ot*CDPK proteins. Orange boxes: Ser/Thr protein kinase domain (PKD), green boxes: EF-hands. (For interpretation of the references to colour in this figure legend, the reader is referred to the web version of this article.)

3.2. Phylogenetic analysis of *Ot*CDPKs

BLASTp searches against non-redundant databases using as query *Ot*CDPK1, collected homologs from green lineage genomes and other photosynthetic organisms belonging to the Stramenopiles or Heterokonta phylum. A phylogenetic analysis showed that *Ot*CDPK1 and *Ot*CDPK2 cluster with algal Clade I as reported by Hamel et al. (2014). Both proteins have the average size of typical CDPKs (~475–550 amino-acid residues) (Supplemental Table 3). On the contrary, *Ot*CDPK3, a larger protein (737 amino-acid residues), groups in Clade IV (Fig. 2) and has a long N-terminal extension (232 amino-acid residues) similar to other prasinophyte CDPKs (*O. lucimarinus*, *Olu*CDPK_42946; *M. pusilla* RCC299, *Mpu*CDPK_58196; *M. pusilla* CCMP1545, *Mpu*CDPK_16149; and *B. prasinos* RCC1105, *Bpr*CDPK_02g01830) (Supplemental Table 3).

Similar tree topologies were obtained when the phylogenetic analysis was performed using full-length sequences or lacking the N-terminus extension (data not shown). A comparative sequence analysis of *Ot*CDPK typical domains with those of other unicellular algae and characterised plant CDPKs showed that they are highly conserved in the green lineage (Supplemental Table 3). Mamiellales contain two or three putative CDPKs that have the typical domains (Figs. 3 and 4). This low number of CDPK isoforms seems to be sufficient to fulfil their role of directly sensing, responding, and translating Ca^{2+} signals due to environmental changes in aquatic habitats. It is likely CDPKs have continued to evolve from the common ancestor of chlorophytes (independently from plant CDPKs) and further gene duplications might give rise to atypical CDPKs or to the appearance of long N-terminal in prasinophytes.

3.3. *OtCDPK1* encodes a CDPK protein

The three putative *OtCDPK* genes are transcribed in cells grown under standard culture conditions (Supplemental Fig. 3). We functionally characterised *OtCDPK1*, the encoding sequence of a putative cytosolyc isoform (Supplemental Table 2), by heterologous expression in *E. coli* cells, immunocharacterization, and further determination of calcium-dependent kinase activity of the resulting recombinant protein (His_6:*Ot*CDPK1) (Fig. 5). This is the first report of a functional CDPK from a prasinophyte, an algal group that diverged earlier in the green lineage.

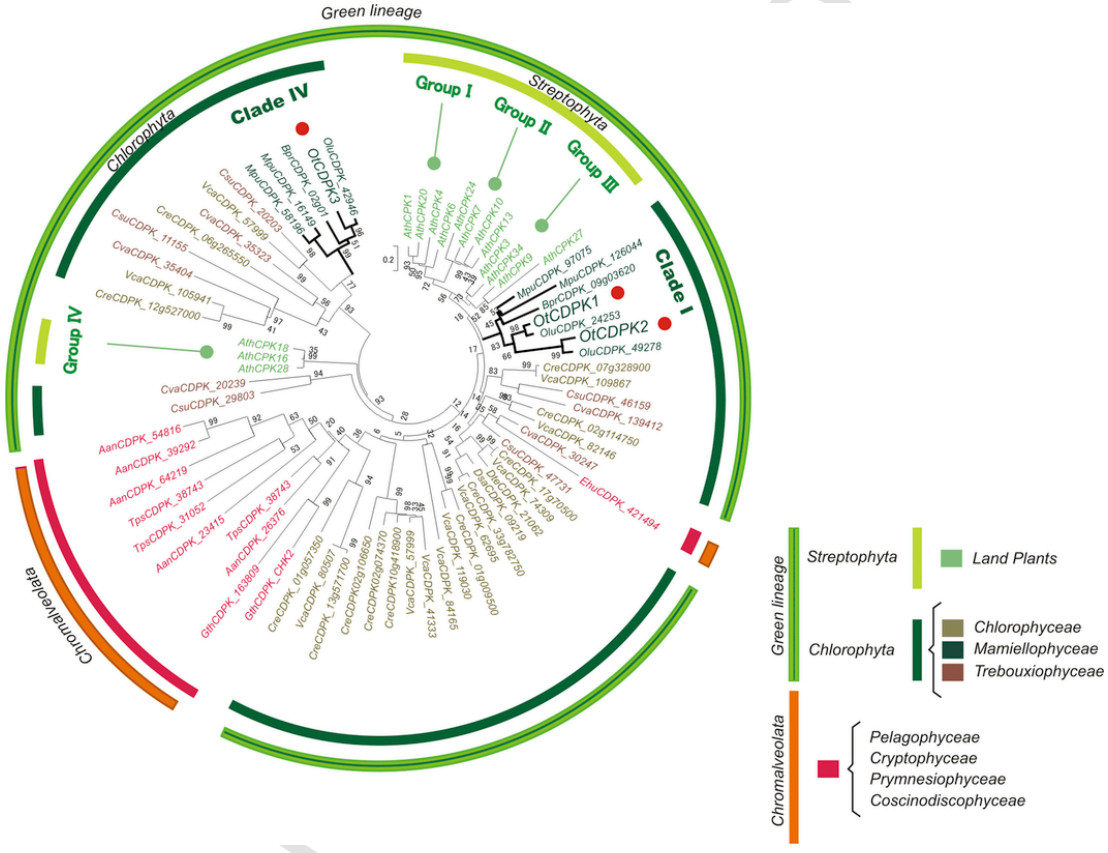

Fig. 2. Relationship among CDPKs from Prasinophyceae and representative CDPKs from green algae and land plants. Full-length sequences encoding CDPKs from members of the class Mamiellophyceae [*Ostreococcus tauri* (*Ot*CDPK1, *Ot*CDPK2 and *Ot*CDPK3 are marked with red circles), *O. lucimarinus* (*Olu*CDPK_42946, *Olu*CDPK_49278, and *Olu*CDPK_24253), *Bathycoccus prasinos* (*Bpr*CDPK_02g01 and *Bpr*CDPK_09g03620), *Micromonas pusilla* RCC299 (*Mpu*CDPK_97075 and *Mpu*CDPK_58196), and *M. pusilla* CCMP1545 (*Mpu*CDPK_126044 and *Mpu*CDPK_16149)], from green algae belonging to Chlorophyceae [*Coccomyxa subellipsoidea* (*Csu*CDPKs), *Volvox carteri* (VcaCDPKs), *Chlorella variabilis* (*Cva*CDPKs), *Chlamydomonas reindhartii*, (*Cre*CDPKs) and *Dunaliella salina* (*Dsa*CDPKs)], and from *Arabidopsis thaliana* (*Ath*CPKs) were included in this analysis. Accession numbers are in Supplemental Table 3. *A. thaliana* CDPK sequences cluster in four groups (I to IV) as reported by Hamel et al. (2014). Sequences were aligned with ClustalW. Resulting alignments were submitted to MEGA5 software to generate a neighbour-joining tree derived from 5000 replicates. As a comparison, we added Chromalveolata CDPK sequences since many chromalveolates were considered among plants because of their photosynthetic ability. (For interpretation of the references to colour in this figure legend, the reader is referred to the web version of this article.)

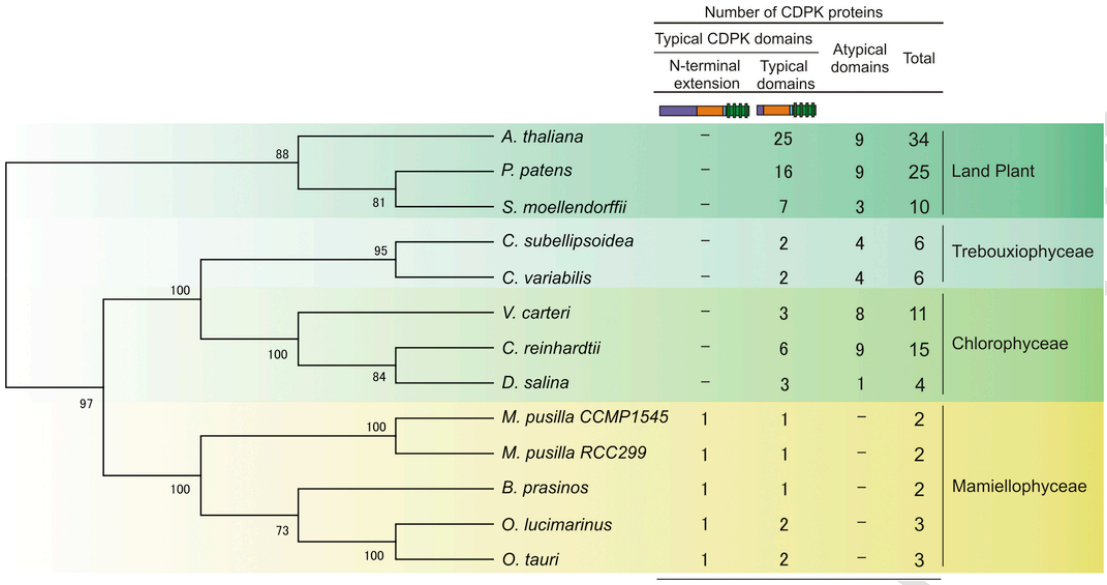

Fig. 3. Relationship between representative green lineage members and their corresponding CDPK structures. Full-length *18S rRNA* sequences [*A. thaliana* (X16077), *P. patens* (X80986), *S. moellendorffii* (X83520), *C. subellipsoidea* (KF673374), *C. variabilis* (Ab260893), *V. carteri* (X53904), *C. reinhardtii* (JN903984), *D. salina* (AF506698), *M. pusilla* CCMP1545 (AY954994), *M. pusilla* RCC299 (DQ025753), *B. prasinos* (AY425315), *O. lucimarinus* (AY329636), *O. tauri* (Y15814)] were aligned with ClustalW and submitted to the MEGA5 software to generate a neighbour-joining tree derived from 1000 replicates (on the left). The number of CDPK sequences retrieved from fully sequenced genomes, as well as the protein structures are shown on the right. CDPKs from *D. salina* were retrieved from https://phytozome.jgi.doe.gov. (For interpretation of the references to colour in this figure legend, the reader is referred to the web version of this article.)

3.4. Effect of nitrogen depletion on OtCDPKs expression

In plants, CDPKs have been reported to be involved in nitrogen assimilation and in several stress signalling pathways (Asano et al., 2010). However, very few studies deal with sensing, uptake, and assimilation of inorganic and organic nitrogen in marine microorganisms (Berg et al., 2008). For the marine phytoplankton, responsible for ocean primary production, nitrogen is often considered a limiting resource (Falkowski, 1997). Thus, we investigated *OtCDPK*s expression in *Ostreococcus* cells grown in Keller medium and then transferred to a nitrogen deficient medium. As shown in Fig. 6, the transcription of the three *OtCDPK*s is up-regulated in response to nitrogen starvation. A similar response has been reported in the freshwater model alga *C. reinhardtii* (Chlorophyceae) (Motiwalla et al., 2014). In fact, the most extensive study on nitrate acquisition and regulation was carried out on *Chlamydomonas* (Sanz-Luque et al., 2015). External nitrate is incorporated by nitrate/nitrite transporters (NRT2), which require a two component high affinity nitrate transport system second protein (NAR2) anchored to the membrane by a transmembrane domain. Inside the cell, nitrate is reduced to nitrite by the action of the enzyme nitrate reductase, which requires among other prosthetic groups, molybdenum cofactor. Interestingly, some NRT2 proteins are two-component systems, mechanisms that allow organisms to sense and respond to changes in environmental conditions. In Micromonas (prasinophytes order Mamiellales), the expression of the putative low-/dual-affinity NRT transporters were sensitive to changes during N-depletion. All gene targets were up-regulated during the N-starvation period (McDonald et al., 2010). Findings in *Chlamydomonas* could be extrapolated to *O. tauri*, since the complete cluster for nitrate acquisition (NAR1-NIA1-NII1-Cyt-b5R-NAR2-NRT2-MOT1-CNX2CNX5) is present in the genome (Derelle et al., 2006; Sanz-Luque et al., 2015).

Our data in *O. tauri* strongly support a role for *Ot*CDPKs in sensing the nitrogen status in the marine environment. *Ostreococcus* may respond to changes in nitrate concentration through a stimulus-response coupling mechanism utilizing CDPKs for signal transduction. One of the most difficult and important challenges is to identify the *Ot*CDPKs *in-vivo* targets.

4. Conclusion

The occurrence of functional CDPKs in Mamillophyceae, a group that includes photosynthetic picoplanktonic species placed in the base of the green lineage, supports the ancestral origin of a Ca^{2+}-dependent signalling pathway. Interestingly, the adaptation to aquatic environmental changes, such as nitrogen depletion, could be sensed by a low number of CDPKs (two or three), according to the sequences retrieved from *O. tauri*, *O. lucimarinus*, *B. prasinos*, and *M. pusilla* genomes. Interestingly, the transcription of the three *OtCDPK* genes is up-regulated after nitrogen starvation, suggesting a major role for them in the signal transduction pathway of the low-nitrogen stress response. We conclude that CDPKs may be key actors in biogeochemical cycling in oligotrophic areas, and consequently, in the ocean primary productivity. *O. tauri* could be a good model to study green alga Ca^{2+}-dependent signalling in the marine picophytoplankton.

Authors' contributions

G.C., G.M-N., and G.L.S. designed research; G.C., D.S., G.M-N., and G.L.S. performed research; G.C., G.M-N., and G.L.S. analyzed data; G.C. and G.L.S. wrote the paper.

Acknowledgements

Authors are indebted to C. Fernández (CIC, Prov. de Buenos Aires) for technical assistance. This work was supported by the Consejo Nacional de Investigaciones Científicas y Técnicas (CONICET, PIP 134); Fundación para Investigaciones Biológicas Aplicadas (FIBA, 2012–2015); Agencia Nacional de Promoción Científica y

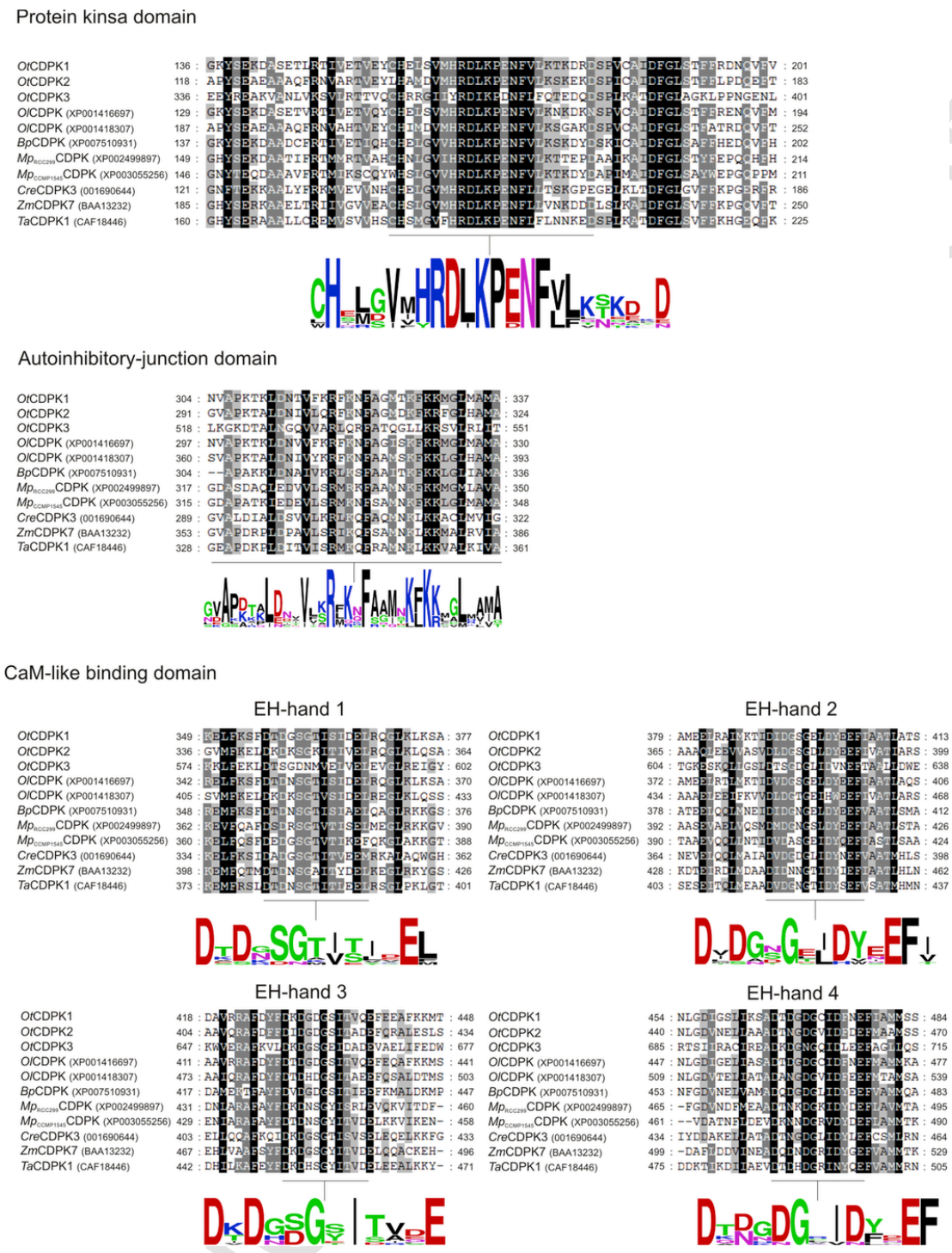

Fig. 4. Comparison of CDPK conserved domains in Mamiellophyceae (the largest clade of prasinophytes), Chlorophyceae and land plants. Multiple alignments of the CDPK domain sequences (protein kinase domain, autoinhibitory-junction domain and EF-hands) were performed with ClustalW. WebLogos were generated from the canonical motif of each domain. *Ot*CDPK1 amino-acid deduced sequence was compared with those of other prasinophyte CDPKs [*Ot*CDPK2 and *Ot*CDPK3 from *O. tauri*; *Ol*CDPKs (XP_001416697 and XP_001418307) from *O. lucimarinus*; *Bp*CDPK (XP_007510931) from *B. prasinos*; *Mp*CDPKs (XP_002499897 and XP_003055256) from *M. pusilla*], with the Chlorophyceae CreCDPK3 (XP_001690644) from *C. reindhartii*, and with the plant CDPKs *Zm*CDPK (BAA13232) from *Z. mays* and *Ta*CDPK1 (Q6KCK6) from *T. aestivum*.

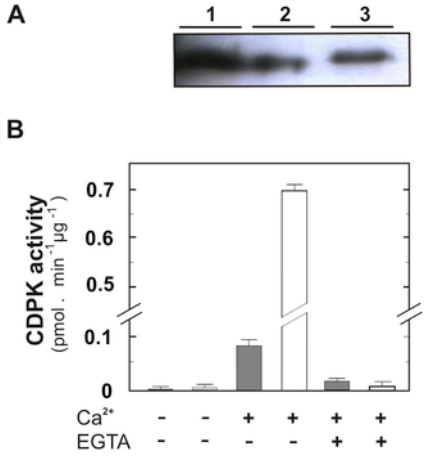

Fig. 5. Functional characterisation of *Ot*CDPK1 by heterologous expression in *E. coli*. **A)** Immunodetection of His_6-tagged recombinant OtCDPK1. Protein extracts from bacteria transformed with a construct to express OtCDPK1 were resolved on 10% SDS-PAGE and immunoanalysed with His-tag antibodies. Concentrated supernatant of total protein extract, (lane 1), purified His_6-tagged *Ot*CDPK1 (lane 2), and recombinant potato CDPK (StCDPK2), positive control, (lane 3). **B)** *Ot*CDPK1 activity determination. Aliquots from bacterial crude extract (grey bars) and purified His_6-tagged *Ot*CDPK1 (white bars) were incubated with [γ-^{32}P]ATP at room temperature for 30 min, in the presence of Syntide-2 peptide (exogenous substrate), and with (+) or without (−) addition of 100 µM Ca^{2+} or 1 mM EGTA (Ca^{2+} chelator). Enzyme activity was quantified on P-81 paper in a scintillation counter and protein content (5.8 and 0.24 µg µL^{-1} in the crude extract and purified recombinant protein, respectively) was determined by Bradford (1976). Specific enzyme activity was expressed as picomoles of ^{32}P incorporated per min per µg of protein. Error bars indicate the standard errors of the means (n = 3).

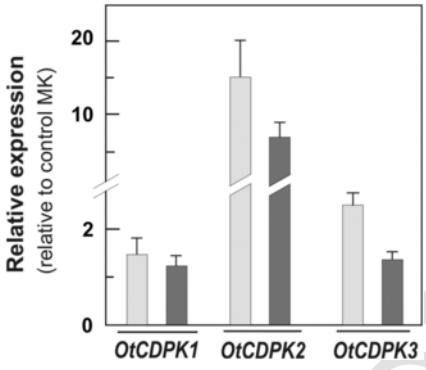

Fig. 6. Effect of nitrogen deprivation on *OtCDPK*s expression. Total RNA from cells cultured in Keller medium (MK, control) or harvested after 2 (light grey bars) or 4 h (dark grey bars) of nitrogen starvation were used to conduct expression analysis by qRT-PCR. Quantitative PCR is indicated as fold-change of experimental treatments relative to control samples (MK) determined by relative standard curve method between the experimental conditions. *OtGAPDH* (GenBank accession number CAL52398) was used as internal control. Mean values and SDs were obtained from two replicates.

Tecnológica (PICT 2012-1288); and Universidad Nacional de Mar del Plata (EXA743/15).

Appendix A. Supplementary data

Supplementary data related to this article can be found at http://dx.doi.org/10.1016/j.plaphy.2017.07.009.

References

Asano, T., Wakayama, M., Aoki, N., Komatsu, S., Ichikawa, H., Hirochika, H., Ohsugi, R., 2010. Overexpression of a calcium-dependent protein kinase gene enhances growth of rice under low-nitrogen conditions. Plant Biotech. 27, 369–373.
Berg, G.M., Shrager, J., Glöckner, G., Arrigo, K.R., Grossman, A.R., 2008. Understanding nitrogen limitation in Aureococcus anophagefferens (Pelagophyceae) through cDNA and qRT-PCR analysis. J. Phycol. 44, 1235–1249.
Billker, O., Lourido, S., Sibley, L.D., 2009. Calcium-dependent signaling and kinases in Apicomplexan parasites. Cell Host Microbe 5, 612–622.
Bodén, M., Hawkins, J., 2005. Prediction of subcellular localization using sequence-biased recurrent networks. Bioinformatics 21, 2279–2286.
Bologna, G., Yvon, C., Duvaud, S., Veuthey, A.L., 2004. N-terminal myristoylation predictions by ensembles of neural networks. Proteomics 4, 1626–1632.
Bradford, M.M., 1976. A rapid and sensitive method for the quantitation of microgram quantities of protein utilizing the principle of protein-dye binding. Anal. Biochem. 7, 248–254.
Cheng, S.H., Willmann, M.R., Chen, H.C., Sheen, J., 2002. Calcium signaling through protein kinases. The Arabidopsis calcium-dependent protein kinase gene family. Plant Physiol. 129, 469–485.
Chico, J.M., Raíces, M., Téllez-Iñón, M.T., Ulloa, R.M., 2002. A calcium-dependent protein kinase is systemically induced upon wounding in tomato plants. Plant Physiol. 128, 256–270.
Claros, M.G., Vincens, P., 1996. Computational method to predict mitochondrially imported proteins and their targeting sequences. Eur. J. Biochem. 241, 779–786.
Crooks, G.E., Hon, G., Chandonia, J.M., Brenner, S.E., 2004. WebLogo: a sequence logo generator. Genome Res. 14, 1188–1190.
de Castro, E., Sigrist, C.J.A., Gattiker, A., Bulliard, V., Langendijk-Genevaux, P.S., Gasteiger, E., Bairoch, A., Hulo, N., 2006. ScanProsite: detection of PROSITE signature matches and ProRule-associated functional and structural residues in proteins. Nucleic Acids Res. 34, W362–W365.
Delaux, P.M., Radhakrishnan, G.V., Jayaraman, D., Cheema, J., Malbreil, M., Volkening, J.D., Sekimoto, H., Nishiyama, T., Melkonian, M., Pokorny, L., Rothfels, C.J., Sederoff, H.W., Stevenson, D.W., Surek, B., Zhang, Y., Sussman, M.R., Dunand, C., Morris, R.J., Roux, C., Wong, G.K.S., Oldroyd, G.E.D., Anéa, J.M., 2015. Algal ancestor of land plants was preadapted for symbiosis. Proc. Natl. Acad. Sci. U. S. A. 112, 13390–13395.
Derelle, E., Ferraz, C., Rombauts, S., Rouzé, P., Worden, A.Z., Robbens, S., Partensky, F., Degroeve, S., Echeynié, S., Cooke, R., Saeys, Y., Wuyts, J., Jabbari, K., Bowler, C., Panaud, O., Piégu, B., Ball, S.G., Ral, J.P., Bouget, F.Y., Piganeau, G., de Baets, B., Picard, A., Delseny, M., Demaille, J., Van de Peer, Y., Moreau, H., 2006. Genome analysis of the smallest free-living eukaryote Ostreococcus tauri unveils many unique features. Proc. Natl. Acad. Sci. U. S. A. 103, 11647–11652.
Emanuelsson, O., Nielsen, H., von Heijne, G., 1999. ChloroP, a neural network-based method for predicting chloroplast transit peptides and their cleavage sites. Protein Sci. 8, 978–984.
Emanuelsson, O., Brunak, S., von Heijne, G., Nielsen, H., 2007. Locating proteins in the cell using TargetP, SignalP and related tools. Nat. Protoc. 2, 953–971.
Falkowski, P.G., 1997. Evolution of the nitrogen cycle and its influence on the biological sequestration of CO_2 in the ocean. Nature 387, 272–275.
Frattini, M., Morello, L., Breviario, D., 1999. Rice calcium-dependent protein kinase isoforms OsCDPK2 and OsCDPK11 show different responses to light and different expression patterns during seed development. Plant Mol. Biol. 41, 753–764.
Guo, Y.L., Roux, S.J., 1990. Partial purification and characterization of a Ca^{2+}-dependent protein kinase from the green alga Dunaliella salina. Plant Physiol. 94, 143–150.
Hamel, L.P., Sheen, J., Séguin, A., 2014. Ancient signals: comparative genomics of green plant CDPKs. Trends Plant Sci. 19, 79–89.
Harmon, A.C., Gribskov, M., Harper, J.F., 2000. CDPKs: a kinase for every Ca^{2+} signal?. Trends Plant Sci. 5, 154–159.
Harper, J.F., Sussman, M.R., Schaller, G.E., Putnam-Evans, C., Charbonneau, H., Harmon, A.C., 1991. A calcium-dependent protein kinase with a regulatory domain similar to calmodulin. Science 252, 951–954.
Hawkins, J., Bodén, M., 2006. Detecting and sorting targeting peptides with neural networks and support vector machines. J. Bioinform. Comput. Biol. 4, 1–18.
Hindle, M.M., Martin, S.F., Noordally, Z.B., van Ooijen, G., Barrios-Llerena, M.E., Simpson, T.I., Le Bihan, T., Millar, A.J., 2014. The reduced kinome of Ostreococcus tauri: core eukaryotic signalling components in a tractable model species. BMC Genomics 15, 640.

Horton, P., Park, K.J., Obayashi, T., Fujita, N., Harada, H., Adams-Collier, C.J., Nakai, K., 2007. WoLF PSORT: protein localization predictor. Nucleic Acids Res. 35, W585–W587.

Hu, Z., Lv, X., Xia, X., Zhou, J., Shi, K., Yu, J., Zhou, Y., 2016. Genome-wide identification and expression analysis of calcium-dependent protein kinase in tomato. Front. Plant Sci. Apr. 8 (7), 469. http://dx.doi.org/10.3389/fpls.2016.00469, eCollection 2016.

Keller, M.D., Selvin, R.C., Claus, W., Guillard, R.R.L., 1987. Media for the culture of oceanic ultraphytoplankton. J. Phycol. 23, 633–638.

Kumar, K.S., Ullanat, R., Jayabaskaran, C., 2004. Molecular cloning, characterization, tissue-specific and phytohormone-induced expression of calcium-dependent protein kinase gene in cucumber (Cucumis sativus L.). J. Plant Physiol. 161, 1061–1071.

Leliaert, F., Smith, D.R., Moreau, H., Herron, M., Verbruggen, H., Delwiche, C.F., De Clerck, O., 2012. Phylogeny and molecular evolution of the green algae. Crit. Rev. Plant Sci. 31, 1–46.

Li, W.K.W., 1994. Primary productivity of prochlorophytes, cyanobacteria, and eukaryotic ultraphytoplankton: measurements from cytometric sorting. Limnol. Oceanogr. 39, 169–175.

Liang, Y., Pan, J., 2013. Regulation of flagellar biogenesis by a calcium dependent protein kinase in Chlamydomonas reinhardtii. PLoS One 8, e69902.

McDonald, S.M., Plant, J.N., Worden, A.Z., 2010. The mixed lineage nature of nitrogen transport and assimilation in marine eukaryotic phytoplankton: a case study of micromonas. Mol. Biol. Evol. 27, 2268–2283.

Martín, M.L., Busconi, L., 2001. A rice membrane-bound calcium-dependent protein kinase is activated in response to low temperature. Plant Phys. 125, 1442–1449.

Martínez-Noël, G., Nagaraj, V.J., Caló, G., Wiemken, A., Pontis, H.G., 2007. Sucrose regulated expression of a Ca^{2+}-dependent protein kinase (TaCDPK1) gene in excised leaves of wheat. Plant Physiol. Biochem. 45, 410–419.

Mohanta, T.K., Kumar, P., Hanhong, B., 2017. Genomics and evolutionary aspect of calcium signaling event in calmodulin and calmodulin-like proteins in plants. BMC Plant Biol. 17, 38. http://dx.doi.org/10.1186/s12870-017-0989-3.

Motiwalla, M.J., Sequeira, M.P., D'Souza, J.S., 2014. Two calcium-dependent protein kinases from Chlamydomonas reinhardtii are transcriptionally regulated by nutrient starvation. Plant Signal. Behav. 9, e27969.

Pierleoni, A., Martelli, P.L., Fariselli, P., Casadio, R., 2006. BaCelLo: a balanced subcellular localization predictor. Bioinformatics 22, e408–e416.

Pinontoan, R., Yuasa, T., Anderca, M.I., Matsuoka, T., Uozumi, N., Mori, H., Muto, S., 2000. Cloning of a cDNA encoding a 66-kDa Ca^{2+}-dependent protein kinase (CDPK) from Dunaliella tertiolecta (chlorophyta). J. Phycol. 36, 545–552.

Ren, J., Wen, L., Gao, X., Jin, C., Xue, Y., Yao, X., 2008. CSS-Palm 2.0: an updated software for palmitoylation sites prediction. Protein Eng. Des. Sel. 21, 639–644.

Sanders, D., Pelloux, J., Brownlee, C., Harper, J.F., 2002. Calcium at the cross roads of signaling. Plant Cell S401–S417.

Sanz-Luque, E., Chamizo-Ampudia, A., Llamas, A., Galvan, A., Fernandez, E., 2015. Understanding nitrate assimilation and its regulation in microalgae. Front. Plant Sci. 6, 899. http://dx.doi.org/10.3389/fpls.2015.00899.

Schulz, P., Herde, M., Romeis, T., 2013. Calcium-dependent protein kinases: hubs in plant stress signaling and development. Plant Physiol. 163, 523–530.

Siderius, M., Henskens, H., Porto-leBlanche, A., van Himbergen, J., Musgrave, A., Haring, M., 1997. Characterisation and cloning of a calmodulin-like domain protein kinase from Chlamydomonas moewusii (Gerloff). Planta 202, 76–84.

Simeunovic, A., Mair, A., Wurzinger, B., Teige, M., 2016. Know where your clients are: subcellular localization and targets of calcium-dependent protein kinases. J. Exp. Bot. 67, 3855–3872.

Sugiyama, K., Mori, I.C., Takahashi, K., Muto, S., Shihira-Ishikawa, I., 2000. A calcium-dependent protein kinase functions in wound healing in Ventricaria ventricosa (Chlorophyta). J. Phycol. 36, 1145–1152.

Tamura, K., Peterson, D., Peterson, N., Stecher, G., Nei, M., Kumar, S., 2011. MEGA5: molecular evolutionary genetics analysis using maximum likelihood, evolutionary distance, and maximum parsimony methods. Mol. Biol. Evol. 28, 2731–2739.

Tsai, T.M., Chen, Y.R., Kao, T.W., Tsay, W.S., Wu, C.P., Huang, D.D., Chen, W.H., Chang, C.C., Huang, H.J., 2007. PaCDPK1, a gene encoding calcium-dependent protein kinase from orchid, Phalaenopsis amabilis, is induced by cold, wounding, and pathogen challenge. Plant Cell Rep. 26, 1899–1908.

Wan, B., Lin, Y., Mou, T., 2007. Expression of rice Ca^{2+}-dependent protein kinases (CDPKs) genes under different environmental stresses. FEBS Lett. 581, 1179–1189.

Wang, B., Yeun, L.H., Xue, J.Y., Liu, Y., Ané, J.M., Qiu, Y.L., 2010. Presence of three mycorrhizal genes in the common ancestor of land plants suggests a key role of mycorrhizas in the colonization of land by plants. New Phytol. 186, 514–525.

Ye, S., Wang, L., Xie, W., Wan, B., Li, X., Lin, Y., 2009. Expression profile of calcium-dependent protein kinase (CDPKs) genes during the whole lifespan and under phytohormone treatment conditions in rice (Oryza sativa L. ssp. indica). Plant Mol. Biol. 70, 311–325.

Yuasa, T., Muto, S., 1992. Ca^{2+}-dependent protein kinase from the halotolerant green alga Dunaliella tertiolecta: partial purification and Ca^{2+}-dependent association of the enzyme to the microsomes. Arch. Biochem. Biophys. 296, 175–182.

Yuasa, T., Takahashi, K., Muto, S., 1995. Purification and characterization of a Ca^{2+}-dependent protein kinase from the halotolerant green alga Dunaliella tertiolecta. Plant Cell Physiol. 36, 699–708.

Yuasa, T., Hashimoto, H., 2006. A Calcium-Dependent Protein Kinase (CDPK) in the unicellular green alga Closterium ehrenbergii. Microbes. Environ. 21, 278–283.

Zeng, H., Zhang, Y., Zhang, X., Pi, E., Zhu, Y., 2017. Analysis of EF-hand proteins in soybean genome suggests their potential roles in environmental and nutritional stress signaling. Front. Plant Sci. 8, 877–891.